ELSEVIER

Raman Spectroscopy of C–S–H, Tobermorite, and Jennite

R. James Kirkpatrick,*† J.L. Yarger,** Paul F. McMillan,** Ping Yu,†‡ and Xiandong Cong*†

**Department of Geology, †ACBM Center, and ‡Department of Materials Science and Engineering, University of Illinois, Urbana, Illinois and **Department of Chemistry, Arizona State University, Tempe, Arizona*

Raman spectra of single-phase calcium-silicate hydrate (C–S–H) samples with C/S ratios between 0.88 and 1.45 are consistent with a defect tobermorite model for the structure of these materials, in agreement with previously published nuclear magnetic resonance (NMR) spectroscopic data for the same samples. The Raman spectra of C–S–H samples with C/S ratios <1.0 are very similar to those of 14Å tobermorite. Those of C–S–H samples with C/S ratios ⩾1.0 show substantial concentrations of both Q^1 and Q^2 Si sites and indicate the possible presence of jennite-like environments. Raman spectroscopy, like infrared and NMR, is a probe of local structure on the atomic nearest neighbor and next-nearest neighbor scale, and thus provides significantly different information than diffraction methods. The Raman spectra of the C–S–H have a rich structure and contain peaks for Si–O stretching, Si–O–Si bending, internal deformation of the Si–O tetrahedra and Ca–O polyhedra, and characteristic peaks at lower frequencies. The spectra of jennite and 14Å tobermorite are quite similar, confirming the result from NMR spectroscopy that jennite has dominantly Q^2 polymerization. The Raman spectra of 11Å and 14Å tobermorite are also similar, although our sample of 11Å tobermorite has a significant concentration of Q^3 Si sites, which indicates cross-linking of the chains. ADVANCED CEMENT BASED MATERIALS, 1997, 5, 93–99. *© 1997 Elsevier Science Ltd.*

KEY WORDS: Calcium-silicate hydrate, C-S-H, Spectroscopy, Raman spectroscopy, Cement chemistry, Cement mineralogy

Calcium-silicate hydrate (C–S–H) is the primary binding phase in Portland cements, but because it is poorly crystalline or X-ray amorphous, its structure is not fully understood. Recent nuclear magnetic resonance (NMR) and X-ray absorption spectroscopy of single-phase C–S–H and hydrated Portland cement samples has improved understanding of this material considerably [1–15], but important questions remain about its structure, especially that of samples with relatively large CaO/SiO_2 (C/S) ratios. The C–S–H structure has long been thought to be related to those of tobermorite and jennite [16–18], although the structure of jennite has not been solved by diffraction methods. We have recently proposed a conceptual model of C–S–H structure based on tobermorite, the so-called defect-tobermorite model [8–12], which is based primarily on ^{29}Si and ^{17}O MAS NMR data.

The primary structural unit of tobermorite is a layer composed of sheets of Ca polyhedra with silicate chains on either side [19]. These silicate chains (Q^2 polymerization, where Q^n indicates n bridging oxygens/tetrahedron) have a drierketten arrangement, in which two of the tetrahedra point toward the Ca sheet, and the other, the bridging tetrahedron, is also linked with the interlayer. These Ca-silicate layers have a net negative layer charge and are held together by Ca atoms in the interlayer region, which also contains water molecules.

In the defect tobermorite model, the variation of the C/S ratio of C–S–H from about 0.8 to about 1.3 is accommodated primarily by omission of tetrahedra (probably the bridging tetrahedra), leading to depolymerization of the silicate chains and to increasing Q^1/Q^2 ratios of >1 for compositions with C/S ratios >1.2. Si–OH linkages are required to be present in C–S–H samples with C/S ratios <1.3, and Ca–OH linkages are required at C/S ratios >1.3.

Based on compositional and powder X-ray diffrection (XRD) data, C–S–H with C/S ratios greater than those of our samples (>1.5–1.6, the compositions found in ordinary Portland cement with no added pozzolans) has been thought to contain tobermorite-like and jennite-like regions, with the proportion of jennite-like regions increasing with age [16–18]. Recent ^{29}Si NMR spectroscopy [11,20] indicates that jennite has mostly Q^2 polymerization, rather than the Q^1 polymerization that dominates C–S–H with large C/S ratios. Taken together, the compositional powder XRD and NMR results indicate that the structure of jennite is probably broadly similar to that of tobermorite with alternating

Address correspondence to: R. James Kirkpatrick, Dept. of Geology, Univ. of Illinois, 1301 W. Green St., Urbana, IL, 61801, U.S.A.

ISSN 1065-7355/97/$17.00
PII S1065-7355(97)00001-1

silicate chains missing. Because of these differences, the structure of the central Ca–O sheet is also likely to be quite different in jennite than in tobermorite. These ideas are also consistent with recent high-resolution transmission electron microscopy of tobermorite and jennite [21]. In this model, the Si–O–Ca linkages of the tobermorite structure that are not present in jennite are replaced with Ca–OH linkages. If this model is correct, jennite can be thought of as a particular kind of defect tobermorite with an ordered array of vacant drierketten chains. Verification of this concept will require detailed X-ray or neutron diffraction study.

There are many potential methods to test and further refine these models of C–S–H, among which vibrational spectroscopy (Raman and infrared) holds considerable promise. This paper presents a comprehensive Raman spectroscopic study of 11Å and 14Å tobermorite, jennite, and single-phase C–S–H with relatively small C/S ratios of 0.88 to 1.45. The results support the defect tobermorite model of the structure of this kind of C–S–H and indicate a substantial increase in the relative concentrations of Q^1 Si-tetrahedra with increasing C/S ratio. They also support the general model for the jennite structure described above and provide some evidence for the presence of some jennite-like environments in C–S–H with C/S ratios >1.0. Previous Raman studies of cement materials have focused primarily on characterization of the crystalline phases in cements [22–25] or on the kinetics of C_3S hydration [26].

Raman Spectroscopy

Raman spectroscopy observes changes in the frequency of laser light due to its interaction with vibrational modes in a crystal or molecule. Thus it is broadly similar to infrared (IR) spectroscopy. Unlike IR spectroscopy, however, the vibrational modes that are most strongly Raman active are those that are related to the greatest change in molecular polarizability, and symmetric vibrational modes tend to be most Raman active. McMillan and Hofmeister [27] provide a useful introduction to the experimental methods and structural interpretation of Raman spectra of minerals. Like NMR spectroscopy, vibrational spectroscopy (Raman and IR) is sensitive to local structure, typically nearest atomic neighbors (NN) and next-nearest atomic neighbor (NNN), and thus does not require the presence of the long-range periodicity needed for diffraction methods. Thus, Raman spectroscopy is especially useful for investigating materials like C–S–H that lack long-range structural order. The structural environments interpreted from the data must, however, be considered only local environments. There is no directly interpretable information concerning structural order at distances greater than a few atomic coordination shells. In principle, the peak areas can with suitable calibration provide quantitative information about the relative abundances of different structural environments [28], and qualitative information about the changes in relative abundance with changing composition is readily available.

There is a large data base of published Raman spectra for crystalline and amorphous materials from which to interpret the spectra presented here. Table 1 summarizes the assignments we use, which are based primarily on the results and interpretations in references 28–35 and references in these papers. The interpretations are also fully consistent with the ^{29}Si NMR results for the model compounds and C–S–H samples [10,11].

Experimental Methods

Samples

The C–S–H samples examined here were either selected from the set of samples we previously examined by ^{29}Si and ^{17}O NMR spectroscopy [10,12] (SEWCS and SCFUM series) or were newly synthesized (95-CSH series). Single phase samples have C/S ratios from 0.88 to

TABLE 1. Frequency ranges and assignments for peaks observed in Raman spectra of C–S–H and related crystalline hydrous Ca-silicates[1]

Frequency or Frequency Range (cm^{-1})	Assignment
1077	Symmetrical C–O stretching in carbonate groups.
800–1080	Symmetrical stretching (SS) of Si–O tetrahedra.
1080	SS of Q^3 tetrahedra.
950–1010	SS of Q^2 tetrahedra.
870–900	SS of Q^1 of tetrahedra.
740	Symmetrical in-plane C–O–C bending in carbonate groups.
600–700	Symmetrical bending (SB) of Si–O–Si linkages (deformation of Ca–O polyhedra may contribute, e.g., E_g mode of portlandite).
650–680	SB involving Q^2 Si tetrahedra.
600–630	SB involving Q^3 Si tetrahedra.
430–540	Internal deformations of Si–O tetrahedra (O–Si–O bending).
300–350	Vibrations involving Ca–O polyhedra, e.g., A_{1g} mode of portlandite.
<280	Complex vibrations, presently not understood. May involve Ca–O polyhedra.

[1]Assignments are based on data in refs 28–35.

1.45, and samples containing C-S-H and portlandite have C/S ratios greater than 1.54. The samples from the SEWCS series were made by hydration of reactive β-C_2S with systematic replacement of the hydration solution to yield the range of compositions. The samples of the SCFUM series were made by reaction of CaO and fumed silica at a water/solid ratio of 100. Samples of the 95-CSH series were specially synthesized for this work using the same methods as for the SEWCS series. 11Å and 14Å tobermorite and jennite were synthesized hydrothermally in Parr bombs and were the same samples we examined by ^{29}Si NMR [11]. All samples were stored in evacuated desiccators but were exposed to air during sample transfer and analysis.

Raman Spectroscopy

The Raman spectra were recorded using an Instruments S.A triple spectrometer (model S3000). For the SEWCS and SCFUM series a photomultiplier tube for scanning mode detection was used. For the 95-CSH series a 600 grooves/mm grating was used for dispersion onto a Princeton Instruments CCD PI-1100 multichannel detector. Spectra of the model compounds were collected using both systems, and both sets of data are shown. The Raman scattering was excited using the 488 nm line from a Coherent Corp. Model 90-5 Ar^+ laser. The laser focusing and collection optics were built around a modified Olympus BH-2 petrographic microscope in a 180° backscattering geometry. In general the spectra collected with the CCD have better signal/noise ratios, but those collected with the photomultiplier tube have less tail from the Rayleigh peak overlapping the low frequency bands. We have interpreted only prominent and reproducible spectral features.

Results and Peak Assignments

General Observations

The Raman spectra of the tobermorites, jennite and the C-S-H samples (Figures 1-3) are quite well resolved and contain a large number of bands from which to make structural interpretations. Our approach to interpreting the spectra is empirical and involves comparison of the frequencies of the observed bands among the model compounds and the C-S-H. This approach is similar to that used previously to successfully interpret Raman spectra of silicate glasses (e.g., refs 28-31). Attempts to fully assign the bands and to determine relevant force constants were unsuccessful, because the crystal structures are disordered and poorly known. The observed bands are somewhat better resolved for the crystalline phases than for the C-S-H. Overall resolution is not as good as for many well crystallized Ca-silicates (e.g., ref 32) but is better than for most Ca-

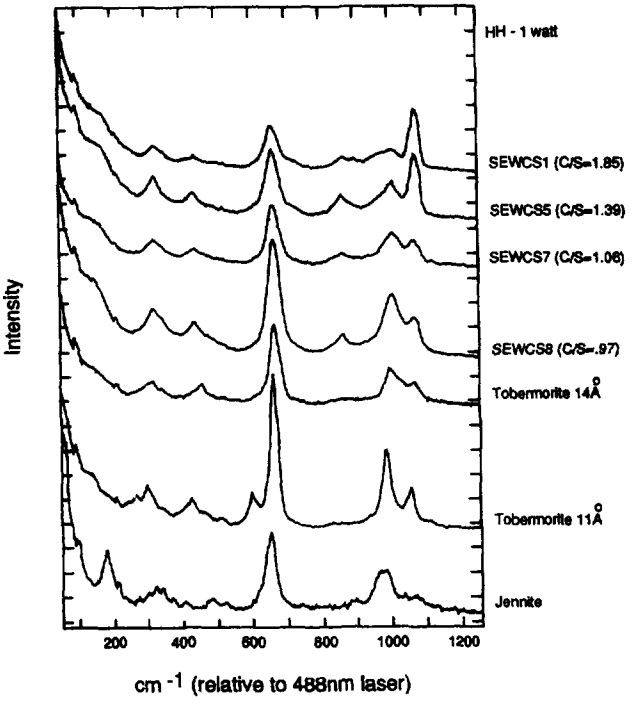

FIGURE 1. Raman spectra of C-S-H samples of the SEWCS series with the labeled C/S ratios, and the Raman spectra of 14Å tobermorite and jennite for comparison. These spectra were collected with the photomultiplier tube.

silicate glasses (e.g., refs 28-31). This observation is the same as for the ^{29}Si NMR spectra of these samples and clearly indicates that the C-S-H samples are structurally less ordered than many crystalline phases but more ordered than glasses.

All the spectra contain a band near 1077 cm^{-1} due to the very Raman-sensitive symmetrical C-O stretching mode, probably in carbonate groups formed from CO_2 absorbed from air. Many of the 95-CSH samples also contain a band near 740 cm^{-1} that is probably caused by in-plane C-O-C bending of the carbonate groups. There is no evidence from optical examination, XRD or the Raman spectra that any of our samples contain crystalline calcite or vaterite as a separate phase. For the C-S-H samples, the intensities of the carbonate bands generally increase with increasing C/S ratio. The extent of carbonation appears to be small, and it is unlikely that it has significantly affected the silicate polymerization.

Crystalline Compounds

11Å TOBERMORITE. The 11 Å tobermorite sample examined here is the "directly synthesized" sample of ref 11. ^{29}Si NMR spectroscopy shows that, like many tobermorites [17,11,20] it is relatively polymerized and contains a substantial concentration of Q^3 Si sites and a small concentration of Q^1 Si sites in addition to the

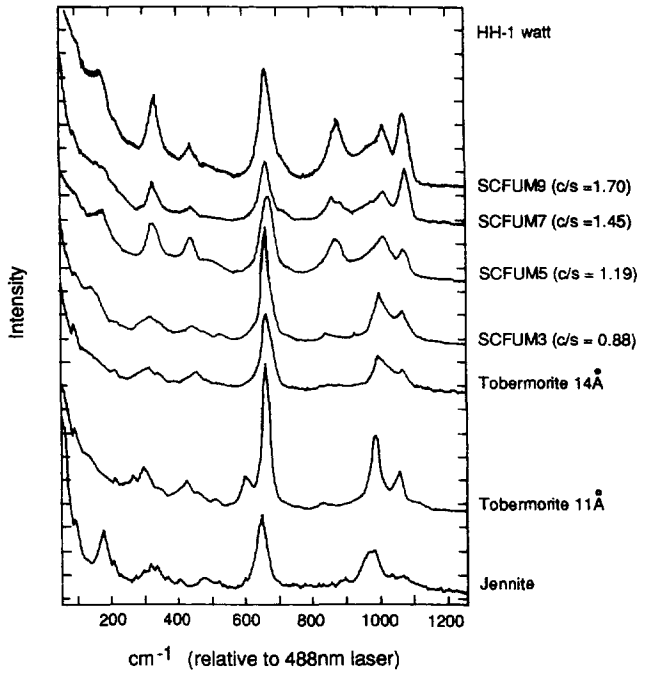

FIGURE 2. Raman spectra of C–S–H samples from the SCFUM series with the labeled C/S ratios, and the Raman spectra of 14Å tobermorite and jennite for comparison. These spectra were collected with the CCD detector.

expected Q^2 sites. The Raman spectrum of this sample is consistent with these results. In the symmetrical Si–O stretching range, the main band is at 1010 cm^{-1} and clearly represents Q^2 sites [28,31,11]. There is also unresolved intensity in the 950–1000 cm^{-1} range that is probably also due to asymmetric Si–O stretching vibrations of Q^2 sites. As for most crystalline compounds, multiple Si–O stretching bands for the same polymerization can be expected [32]. The very low-intensity, broad band at 850 cm^{-1} is assigned to Q^1 sites, as described below for the C–S–H. Signal for these sites is clearly present in the ^{29}Si NMR spectrum of this sample. Raman signal for the Q^3 sites observed by NMR may be present near 1040 cm^{-1}, but this is obscured by the carbonate band. In the Si–O–Si bending region the main peak is at 680 cm^{-1} and is assigned to linkages involving Q^2 tetrahedra [28–32]. Signals caused by bending vibrations (librations) of Ca–OH groups may also contribute in this band [33], but spectra of C–S–H made with deuterated water (data not shown) demonstrate that the main component is Si–O–Si bending. The small peak near 620 cm^{-1} is assigned to Si–O–Si linkages involving Q^3 tetrahedra. It is known [28] that for silicate glasses the frequency of the Si–O–Si bending band increases with decreasing polymerization of the Si-tetrahedra, consistent with this assignment. The band at 450 cm^{-1} is readily assigned to internal deformations of the SiO_4 tetrahedra [32]. This band appears to be asymmetrical to higher frequencies, with intensity extending to approximately 500 cm^{-1}. The band at ca. 320 cm^{-1} can be assigned to OH translational modes comparable to A_{1g} vibrations of portlandite [33]. There are several peaks at frequencies less than 250 cm^{-1} which are on the tail of the Rayleigh peak. These peaks are not well understood and may be associated with motions of the Ca–O polyhedra.

14Å TOBERMORITE. The spectrum of the 14 Å tobermorite is somewhat simpler than that for 11Å tobermorite, and although its structure has not been determined by diffraction methods, many features of the spectrum are readily understood. Powder XRD and NMR spectroscopy confirm that the structure of this sample is similar to 11Å tobermorite but with a larger basal spacing caused by more water molecules in the interlayer [11]. ^{29}Si NMR shows that most of the Si-tetrahedra have Q^2 polymerization, and that less than 5% have Q^1 polymerization [11]. The Raman spectrum is consistent with this result, and the main peak positions are essentially the same as those for 11 Å tobermorite. The main Si–O stretching frequency is at 1005 cm^{-1}, consistent with Q^2 polymerization, and there is only a weak, broad Q^1 band at about 850 cm^{-1}. The Si–O–Si bending peak is at

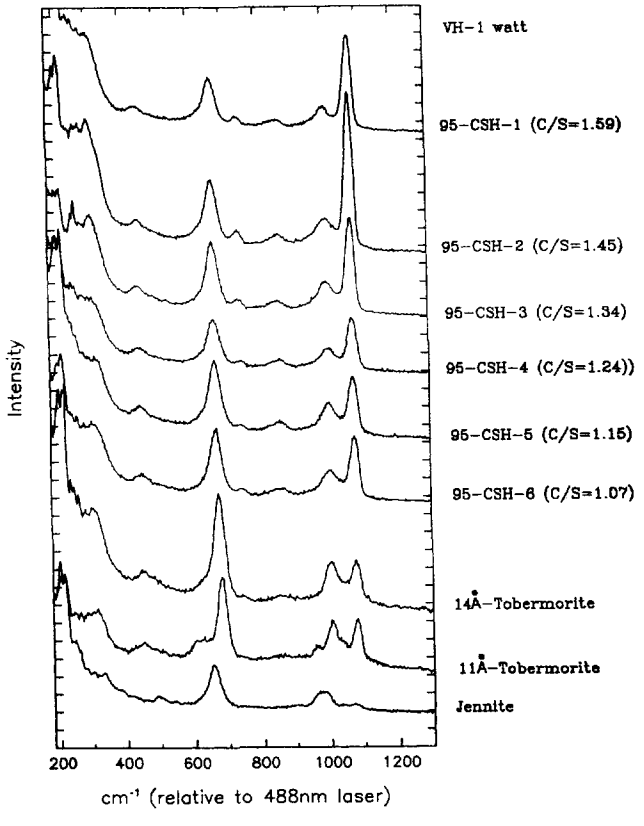

FIGURE 3. Raman spectra of C–S–H samples from the 95-CSH series with the indicated C/S ratios. These spectra were collected with the CCD detector.

675 cm^{-1}. The band for internal vibrations of the Si-tetrahedra is at 450 cm^{-1}, and as for 11 Å tobermorite is asymmetrical with intensity extending to 500 cm^{-1}. The bands at lower frequencies are also essentially the same as for 11 Å tobermorite. The band widths of the 14 Å tobermorite are larger than those of the 11Å tobermorite, which is indicative of greater structural disorder, in agreement with the ^{29}Si NMR results for the samples [11]. Both the tobermorite samples yield a band at 1070 cm^{-1} because of the symmetric stretch of CO_3^{2-} groups in the interlayers. We will describe the assignments and implications of this feature elsewhere.

JENNITE. The spectrum for jennite is quite similar to those of the tobermorites, but the band frequencies are significantly different, providing useful information for comparison to the C-S-H samples. The structure of jennite [36,37] has not been determined by diffraction methods, but powder XRD and ^{29}Si NMR results [11,20,36,37] indicate that it contains chains of silicate tetrahedra with Q^2 polymerization. As described above, its general long-range structure can be thought of as based on that of tobermorite with alternate tetrahedral chains missing and replaced by Ca-OH linkages. Because of the OH for silicate substitution, the Ca-O polyhedra are also likely to be different. The ^{29}Si NMR spectrum of our sample shows the presence Q^2 tetrahedra with a very small peak for Q^1 sites [11]. The Raman spectrum of this sample is fully consistent with this interpretation. The main Si-O stretching frequencies are in a broad band centered at ca. 970 cm^{-1}, lower in frequency than the main analogous band for the tobermorites, but still consistent with Q^2 units. The Si-O-Si bending peak is at 655 cm^{-1}, again slightly lower in frequency than the analogous band for the tobermorites. There is a band at 490 cm^{-1}, analogous to the 450 cm^{-1} band of tobermorites due to internal deformation of the Si-tetrahedra. These two observations indicate that the O-Si-O and Si-O-Si angles are slightly different than in tobermorite. Jennite also has a band at 325 cm^{-1} because of OH translation and several peaks at lower frequencies. The most prominent of these is at 180 cm^{-1} and is not present for the tobermorites. Assignment of this peak is presently uncertain, but given the expected differences in the structures of the central Ca-layer in tobermorite and jennite, it may be caused by vibrations involving Ca-polyhedra that are different than those in tobermorite. The C-O symmetric stretching band at 1077 cm^{-1} is weaker than for the tobermorites, indicating the presence of fewer carbonate groups in this sample.

C-S-H Samples

The Raman spectra of our C-S-H samples (Figures 1-3) are, as expected, very similar to those of the tobermorite and jennite. Band resolution is somewhat less than for the crystalline phases, especially for the Si-O-Si bending band near 665 cm^{-1} of the samples with C/S ratios >1.0.

Si-O STRETCHING REGION. For samples with C/S ratios <1.0, the band for symmetrical Si-O stretching vibrations in Si-tetrahedra is centered at 1005 cm^{-1}, the same frequency as the bands for Q^2 tetrahedra in the tobermorites. With increasing C/S ratio, the dominant Q^2 band remains at this position, but there is increased intensity in the 950–1000 cm^{-1} range, the range for the small peak observed for the 11 Å tobermorite and the Q^2 sites in jennite. Most importantly, the relative intensity of the band for Q^1 tetrahedra centered near 970 cm^{-1} range increases with increasing C/S ratio.

Si-O-Si BENDING REGION. For all the C-S-H samples, the main Si-O-Si bending frequency is at 664–669 cm^{-1}, between the values of the main analogous bands for the tobermorites (675–680 cm^{-1}) and jennite (665 cm^{-1}). There is no systematic change in the position of this band with C/S ratio, but it is broader for samples with C/S ratios >1.0 than for those with smaller C/S ratios. There is never a resolved peak or shoulder at ca. 655 cm^{-1}, the frequency for this peak for jennite, although the peak for most of the samples has intensity in this region. As expected from the lack of Q^3 sites, there is no peak near 620 cm^{-1} which would be indicative of Si-O-Si bending motions involving Q^3 tetrahedra, as observed for the 11Å tobermorite.

400–600 cm^{-1} REGION. The major band in this region for all the C-S-H samples has a maximum at 450 cm^{-1}, the position for the major band in this region for the tobermorites. In addition, some of the samples have a small amount of intensity extending to 500 cm^{-1}. Tobermorite has intensity in this region, and jennite has a band maximum at 490 cm^{-1}. As for the tobermorites and jennite, this peak can be readily assigned to internal deformation of the Si-tetrahedra.

250–400 cm^{-1} REGION. For C-S-H, the major peak in this region is at 325 cm^{-1}, near the positions for the major peaks in this region for the tobermorites and jennite. This frequency is only slightly less than that of the main Raman peak for portlandite at 345 cm^{-1} and is readily assigned to OH translation in all of these phases.

100–250 cm^{-1} REGION. Like tobermorite and jennite, most of the C-S-H samples have intensity in this region, possibly due to Ca^{2+} motions.

Discussion

As for the previously published X-ray diffraction, TEM, ^{29}Si and ^{17}O NMR and Ca X-ray absorption spectroscopy

(XAS) results [1–21,36–37], the Raman results described above clearly demonstrate the similarity of the structures of tobermorite and jennite. They also demonstrate the similarity of the structures of our single-phase C–S–H samples and tobermorite and the importance of depolymerization of the silicate chains (forming Q^1 tetrahedra) to accommodate increasing C/S ratios, in agreement with the ^{29}Si NMR results. Evidence for strong similarity between the structures of our C–S–H samples with high C/S ratios and jennite is lacking, although there is some similar spectral features indicating that jennite-like environments may be present.

The most important evidence for the similarity of our C–S–H and tobermorite from the Raman spectra is that every strong band observed for the 14Å tobermorite is also present for the C–S–H samples at nearly the same frequencies. In addition, however, the band for Si–O stretching in Q^1 tetrahedra is prominent for samples with C/S ratios $\geq$1.0, and its intensity relative to the Q^2 band at 1005 cm^{-1} generally increases with increasing C/S ratio. This observation is fully consistent with the ^{29}Si NMR results and confirms the progressive depolymerization of C–S–H with increasing C/S ratio. The band for Si–O–Si bending involving Q^3 tetrahedra at 600 cm^{-1}, which is clearly present for the 11 Å tobermorite, is not prominently present for the C–S–H samples, consistent with the ^{29}Si NMR observation that those samples with C/S ratios >0.88 do not contain significant concentrations of Q^3 tetrahedra.

Evidence for the general similarity of the C–S–H structure to that of jennite is lacking (e.g., the silicate polymerization of C–S–H with large C/S ratios is dominantly Q^1) [10,11], but there is some Raman evidence for the presence of local jennite-like structures or perhaps jennite-like domains. The strongest such evidence is the intensity for Q^2 sites between 950 and 1000 cm^{-1}. The increase in signal intensity in the 950–1000 cm^{-1} range with increasing C/S ratio is consistent with an increasing abundance of jennite-like Q^2 Si-environments, although the 11 Å tobermorite also has signal in this region. The strong band at 180 cm^{-1} is not observed for the tobermorites, but is present for jennite and C–S–H. The primary structural differences between jennite and tobermorite appear to be missing silicate chains which are replaced by Ca–O–H linkages and consequent changes in the Ca–O polyhedra. Thus, although the origin of this band is not known, it may be associated with vibrations involving Ca-polyhedra with Ca–O–H linkages. One argument against the presence of a large fraction of jennite-like environments in our C–S–H samples is the lack of a significant shift of the Si–O–Si bending band to near 655 cm^{-1} with increasing C/S ratio. If there were large and increasing concentrations of jennite-like sites, we would expect such a shift to occur based on the results for model compounds.

Although Raman spectroscopy, like NMR spectroscopy, does not provide information concerning long-range order, other types of data clearly indicate that C–S–H is a compositionally and structurally heterogeneous material. Powder X-ray diffraction patterns of C–S–H generally contain fewer peaks than those of tobermorite and jennite, and the peaks are broader [10,16–18]. The patterns of samples with C/S ratios of 1 are often quite similar to those of tobermorite, but they typically become less well resolved with increasing C/S ratios above 1.0. Thus, there are unlikely to be ordered tobermorite or jennite domains in C–S–H on a scale larger than a few 10s of nm. Recent ^1H–^{29}Si CPMAS NMR results show that the Q^1 and Q^2 sites in C–S–H are associated with different ^1H reservoirs, suggesting that these sites may not be dominantly co-polymerized [8]. High resolution TEM work [38] on C–S–H from cement pastes shows the presence of domains a few tens of nm across which have varying C/S ratios and lattice spacings that vary continuously between those of tobermorite and jennite. In addition, the domains are separated by similar sized volumes with no resolvable lattice spacings.

What remains unclear from present data is whether the tobermorite-like, jennite-like and Q^1-rich regions occur in the same or separate structural domains, and if they are in separate domains, which ones they are in. The jennite-like Q^2 sites inferred from the Raman spectra, for instance, need not be present in large domains with the jennite structure. If these sites are present, the results probably require only that they be in chains segments with neighboring chain segments missing.

Conclusions

Raman spectra of single-phase C–S–H samples with C/S ratios of 0.79 to 1.45 and C–S–H samples containing portlandite with C/S ratios as large as 1.85 confirm both the similarity of the structure of C–S–H to that of tobermorite and omission of tetrahedra in the silicate chains as a main mechanism for accommodating increases in the C/S ratio in these samples [10,11]. The results also confirm that the structure of jennite is dominated by silicate tetrahedra with Q^2 polymerization [36,37], and that local Q^2 silicate environments similar to those in jennite may also be present in C–S–H. From a local structural standpoint, the defect tobermorite model of C–S–H is conceptually useful, because it allows creation of the full range of silicate environments that occur in C–S–H. C–O stretching and sometimes O–C–O bending bands are present in the spectra indicating the presence of carbonate groups. These modes are very Raman-active, and it is unlikely that the silicate polymerization has been significantly affected by the presence of these impurities.

Acknowledgments

This research was supported by the National Science Foundation Center for Advanced Cement-Based Materials. Prof. J. Francis Young introduced us to the problems of C–S–H structure and has been supportive throughout our work. The initial manuscript was improved significantly by three anonymous reviews.

References

1. Young, J.F. *J. Am. Cer. Soc.* **1988,** C118–C120.
2. Grutzeck, M.; Benesi, A.; Fanning, B. *J. Am. Cer. Soc.* **1989,** *72,* 665–668.
3. Bell, G.M.M.; Bensted, J.; Glasser, F.P.; Lachowski, E.E.; Roberts, D.R.; Taylor, M.J. *Advn. in Cem. Res.* **1990,** *3,* 23–37.
4. Cong, X.-D.; Kirkpatrick, R.J. *Cem. Concrete Res.* **1993,** *23,* 1065–1077.
5. Kirkpatrick, R.J.; Cong, X.-D., in Colombet, P., and Grimmer, A.-R., eds, Application of NMR spectroscopy to Cement Science **1993,** Harwood, Amsterdam.
6. Brough, A.R.; Dobson, C.M.; Richardson, I.G.; Groves, G.W. *J. Am. Cer. Soc.* **1994,** *77,* 593–596.
7. Okada, Y.; Ishida, H.; Mitsuda, T. *J. Am. Cer. Soc.* **1994,** *77,* 765–768.
8. Cong, X.-D.; Kirkpatrick, R.J. *Advn. Cem. Res.* **1995,** *7,* 103–111.
9. Cong, X.-D.; Kirkpatrick, R.J. *Cem. Concrete Res.* **1995,** *25,* 1237–1245.
10. Cong, X.-D.; Kirkpatrick, R.J. *Advn. Cem. Based Materials* **1996,** *3,* 144–156.
11. Cong, X.-D.; Kirkpatrick, R.J. *Advn. Cem. Based Materials* **1996,** *3,* 133–143.
12. Cong, X.-D.; Kirkpatrick, R.J. *J. Am. Cer. Soc.* **1996,** *79,* 1585–1592.
13. Kirkpatrick, R.J.; Brown, G.E.; Xu, N.; Cong, X.-D. *Advn. Cem. Res.* **1997,** *9,* 31–36.
14. Richardson, I.G.; Groves, G.W. *Cem. Concrete Res.* **1992,** *22,* 1001–1010.
15. Richardson, I.G.; Groves, G.W., *Cem. Concrete Res.* **1993,** *23,* 131–138.
16. Taylor, H.F.W. *J. Am. Ceram. Soc.* **1986,** *69,* 464–467.
17. Taylor, H.F.W., *The Chemistry of Cement* Academic Press, London, 1992.
18. Taylor, H.F.W. *J. Advn. Cem. Based Materials* **1993,** *1,* 38–46.
19. Hamid, S.A.; Zeit. Kristallog. **1981,** *154,* 189–198.
20. Komarneni, S.; Roy, D.M.; Fyfe, C.A.; Kennedy, G.J. *J. Cem. Concr. Res.* **1987,** *17,* 891–895.
21. Viehland, D.; Yuan, L.J.; Xu, Z.; Cong, X.-D.; and Kirkpatrick, R.J., submitted, *J. Am. Cer. Soc.*
22. Bensted, J. *J. Am. Ceram. Soc.* **1976,** *59,* 140–143.
23. Conjeaud, M.; Boyer, H. *Cem. Concr. Res.* **1980,** *10,* 61–70.
24. Ghosh, S.N.; Handoo, S.K. *Cem. Concr. Res.* **1980,** *10,* 771–782.
25. Dyer, C.D.; Hendra, P.J.; Forsling, W. *Spectrochimica Acta* **1993,** *49A,* 715–722.
26. Tarrida, M.; Madon, M.; Le Rolland, B.; Colombet, P. *J. Advn. Cem. Based Materials* **1994,** *2,* 15–20.
27. McMillan, P.; Hofmeister, A.M., in *Spectroscopic Methods in Mineralogy and Geology* Rev. in Mineralogy, v. 18, Hawthorne, F.C., ed., Mineral. Soc. Am. 1988.
28. McMillan, P.; Piriou, B. *Bull. Mineral.* **1983,** *106,* 57–75.
29. McMillan, P. *Amer. Mineral.* **1984,** *69,* 645–659.
30. Kashio, S.; Iguchi, Y.; Goto, T.; Nishina, T.; Fuwa, T. Trans. of the Iron and Steel Inst. of Japan **1980,** *20,* 251–253.
31. Mysen, B.; Finger, L.W.; Virgo, D.; Seifert, F.A. *Amer. Mineralogist* **1982,** *67,* 686–695.
32. Handke, M. *Appl. Spectroscopy* **1986,** *40,* 871–877.
33. Lagarde, P.; Nerenberg, M.; Farge, Y., in Nusimovici, M.A., ed., Phonon: Proc. of the international conference at Rennes, France, Flammarion Sciences, Paris, 1971, 116–120.
34. Padanyi, Z.V., Solid State Communications, 1970, 8, 841.
35. Kubicki, J.D.; Stolper, E.M. Geochim. Cosmochim. Acta **1995,** *57,* 683–698.
36. Carpenter, A.B.; Chalmers, R.A.; Gard, J.A.; Speakman, K.; Taylor, H.F.W. *Amer. Mineralogist* **1966,** *51,* 56–74.
37. Gard, J.A.; Taylor, H.F.W.; Clift, G.; Lorimer, G.W. *Amer. Mineralogist* **1977,** *62,* 365–368.
38. Viehland, D.; Li, J-F.; Yuan, L-J.; Xu, Z. *J. Am. Cer. Soc.* **1996,** *79,* 1731–1744.